

Multi-objective optimization of the thermal and hydraulic design of a heat exchanger of the type shell and tubes

Y. G. Lovella^a, I. Herrera^b, W. De Paepe^c, F. Contino^d, C. Erlich^e, M. Montero Carrero^f, Sara Pinzi^g, María del Pilar Dorado^g

^a Central University "Marta Abreu" de Las Villas, Santa Clara, Cuba, yanielg@uclv.cu

^b Central University "Marta Abreu" de Las Villas, Santa Clara, Cuba, idalbertohm@uclv.edu.cu

^c Vrije Universiteit Brussel, Brussel, Belgium, wdepaepe@vub.ac.be

^d Vrije Universiteit Brussel, Brussel, Belgium, fcontino@vub.ac.be

^e Kungliga Tekniska Högskolan, Stockholm, Sweden, catharina.erlich@energy.kth.se

^f Vrije Universiteit Brussel, Brussel, Belgium, mmontero@vub.ac.be

^gDep. of Physical Chemistry and Applied Thermodynamics, Edificio Leonardo da Vinci, Campus de Rabanales, Universidad de Córdoba, campus de excelencia agroalimentario, ceiA3, 14071 Córdoba, Spain

Abstract:

The extensive use of heat exchangers in the industry makes its optimization be crucial for raising efficiency and energy conservation. In the context of cleaner production and energy sustainability of the industrial sector, energy efficiency is a cornerstone to reduce fuel consumption. In this way the performance of the heat exchanger is a key factor. This work aims to contribute to energy efficiency, for this purpose a multi-objective optimization of the thermal and hydraulic design of heat exchangers of shell and tubes is implemented. A meta-heuristic technic of genetic algorithm, using two fitness functions, number of entransy dissipation and total cost was programed. Finally it is obtained the Pareto front with multiple solutions, these solutions where adjusted to the operating conditions.

Keywords:

Heat Exchanger, Entransy, Generic Algorithm, Meta-Heuristic, Effectiveness, Viscosity.

1. Introduction

The energy efficiency is necessary to achieve a high standard of development, and energy sustainability. Cuba is a developing country and main economic activities are highly depending of fossil fuel, and about 35% of it is imported. The electricity generation is an important consumer of fossil fuels, representing about 32.6% of the total energy demand [1]. Heat exchangers are widely used in many industrial areas, such as power plant, chemical engineering, petroleum refineries, food processing, etc. [2]. According to [3] heat exchanger of shell and tubes are the 35-40% heat exchanger equipment used in the industry. In 2005 in the frame of the program for the improvement of the national electric power system the decentralized power generation was introduced in Cuba. In these power stations the generating units formed by a set internal combustion engine – generator, are grouped in 3 cells. In a cell the fuel oil is fed to the internal combustion engines (ICE) from the fuel treatment unit, where the fuel oil is preheated and centrifuged in order to reduce its viscosity and humidity. The heat used in the fuel treatment unit is recovered from the combustion gases through a heat recovering boiler. Combustion gases could be conveniently bypassed, total or partially, to follow heat demand. The electric power generated is transmitted from the generators to the electricity treatment unit, where the generators are synchronized and the power generation is regulated according to the effective energy demand. Finally the electricity is sent to the electric grid through the exit transformers.

This works focus on the heat exchanger of the fuel treatment unit. As mentioned heat used is provided by a heat recovering boiler, which generate saturated steam in a rage of pressure from 3.2 bar (320 kPa) to 8 bar. The heat exchanger for fuel heating is of the type of shell and tubes,

designed for saturated steam up to a pressure of 8 bar (800 kPa). Optimal fuel heating is a key factor to achieve a high efficiency of the engines, in this way it has been decided to improve the heat exchanger design for present operating conditions. In order to accomplish this task it is implemented multi-objective optimization of the thermal and hydraulic design for this exchanger, adopting as optimization criteria, entransy dissipation [22] and total cost.

2. Thermal and hydraulic designed

In the present sections is showed the principal calculations, for heat transfer and pressure drop, for the exchanger shown in the figure 1. Discussing the thermodynamic procedure and the designing methodology.

2.1. Procedure thermodynamic

The first thermodynamic law, for the heat exchanger according to [4] Eq. (1).

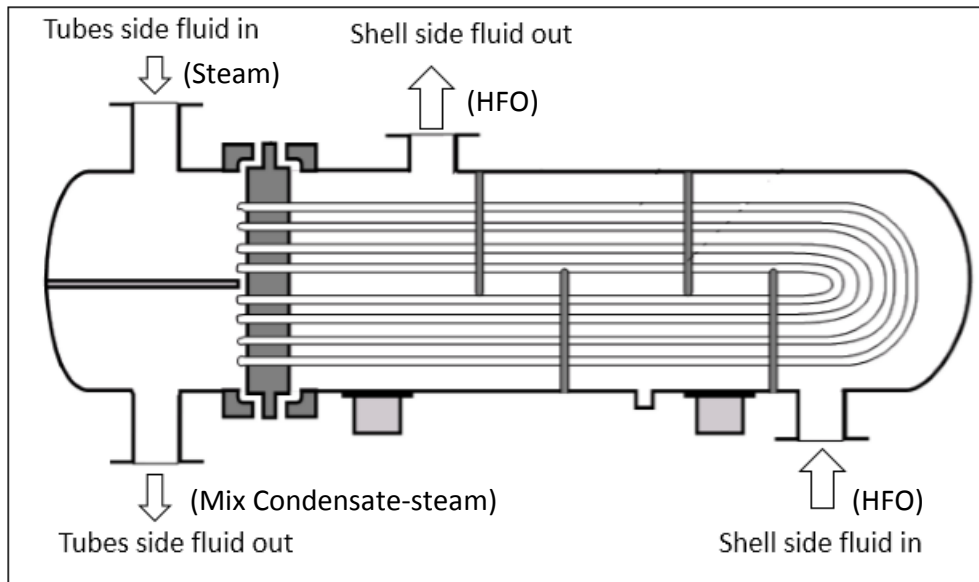


Fig. 1. Diagram of mass flows for U-Tubes heat exchanger.

$$\dot{q} = \dot{m}_h \cdot h_{fg} = \dot{m}_c \cdot C_{p,c} (T_{c,o} - T_{c,i}) \quad (1)$$

$$\dot{q} = C_{min} \cdot \varepsilon \cdot \dot{q}_{max} \quad (2)$$

In [5] is presented the effectiveness and number of transfer unit procedure ($\varepsilon - NTU$), Eq. (3) indicate the effectiveness and Eq. (4) NTU.

$$\varepsilon = \frac{\dot{q}}{\dot{q}_{max}} \quad (3)$$

$$NTU = \frac{U \cdot A_s}{C_{min}} \quad (4)$$

In heat exchanger analysis, it is also convenient to define another dimensionless quantity called the capacity ratio C as.

$$C = \frac{C_{min}}{C_{max}} \quad (5)$$

It can be shown that the effectiveness of a heat exchanger is a function of the number of transfer unit NTU and the capacity ratio.

$$\varepsilon = f(NTU, C) \quad (6)$$

In the previous reference, the correlations are for all configurations of flow and for all capacity ratio, for this case, is assumed the correlations for all heat exchangers with $C = 0$.

2.2. Thermal calculation

The thermal design fundamentally consists in estimating the heat transfer coefficient in the shell side and tube side. For the shell side the Bell-Delaware method is implemented [6]. First it is estimated for pure crossflow conditions the heat transfer for ideal tube bank Eq. (7), the next step is to affect this magnitude by a group of correction coefficients Eq. (8), which are described below.

$$h_{Ideal} = \frac{J_i C_{P,c} G_s \phi}{P_r^{2/3}} \quad (7)$$

$$h_s = h_{Ideal} \cdot J_c \cdot J_L \cdot J_B \cdot J_R \cdot J_S \quad (8)$$

- J_c : This factor take is account baffle cut and central baffle spacing. Its value is 1 for an exchange with no tubes in the window and increase to 1.15 for smalls baffle cut, decrease to 0.65 for large baffle cuts. For good design practice this values is near to 1.
- J_L : Take in count the leakage in Tubes-to-Baffles and Shell-to Baffle (A and B) stream, figure 2. A typical value of this corrector factor is in the range 0.7 to 0.8.
- J_B : Correction factor for the bundle and pass partition bypass (C and F), this factor is about 0.9 to 0.7 depending of tube sheet construction. It can increase from about 0.7 to 0.9 by proper user sealing strips.
- J_R : Correction factor for the large baffle spacing at the inlet and outlet section compare to the central baffle spacing. This factor usually varies from 0.85 to 1.
- J_S : This is a correction factor for advance gradient temperature build-up in laminar flow. This correction is applicable for Reynolds number below 100 and fully effective for Reynolds number below 20; otherwise, it is equal to 1.

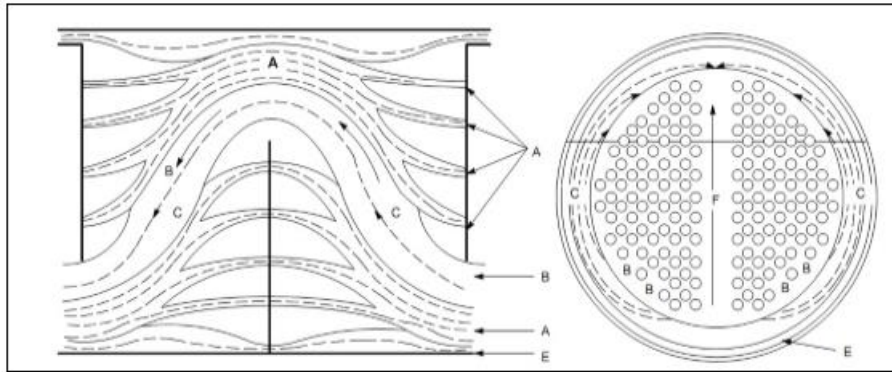


Fig. 2. Diagram of stream for the shell side.

Figure 2 show various streams in order of decreasing influence on thermal effectiveness, those are as follows [6]:

B stream: crossflow stream flowing over the tubes (and fins, if any) between successive windows. This stream is the “desired” stream and is considered fully effective for both heat transfer and pressure drop.

A stream: tube-to-baffle hole leakage stream through the annular clearance between the tubes and baffle holes of a baffle. This stream is created by the pressure difference on the two sides of the baffle. As heat transfer coefficients are very high in the annular spaces, this stream is considered fully effective.

C stream: bundle-to-shell bypass stream through the annular spaces (clearances) between the tube bundle and shell. This bypass flow area exists because the tube holes cannot be punched close to the tubesheet edge, due to the structural strength requirement. The C stream flows between successive baffle windows. This stream is only partially effective for heat transfer, as it contacts only those tubes near the circumference.

E stream: shell-to-baffle leakage stream through the clearance between the edge of a baffle and the shell. This stream is least effective for heat transfer, particularly in laminar flow, because it may not come in contact with any tube.

F stream: tube-pass partition bypass stream through open passages created by tube layout partitions (when placed in the direction of the main crossflow stream) in a multipass unit. This stream is less effective than the A stream because it comes into contact with less heat transfer area per unit volume; however, it is slightly more effective than the C stream. It is listed last because not all exchangers have two or more passes.

To estimate the heat transfer coefficient on the tube side the expressions presented in Eq. (9) and Eq. (10) are used [4].

$$h_t = \frac{g \cdot \rho_l (\rho_l - \rho_v) \cdot k_l^3 \cdot h'_{fg}}{\mu_l (T_{sat} - T_w) \cdot D_i} \quad (9)$$

$$h'_{fg} = h_{fg} + \frac{3}{8} C_{p,l} (T_{sat} - T_w) \quad (10)$$

The application of the Eq. (9) and Eq. (10) in this case, for the calculation of the heat transfer coefficient on the tubes side, results in a numerical error significantly big. However despite the uncertainty we can assure that for this case, due to the condensation process, the heat transfer coefficient on the tubes side is higher than on the shell side. As shown in figure 1, fuel oil flow on shell side, being the controlling film, due to the high viscosity of this substance and because no phase change occur. The global heat transfer coefficient is strongly determined for the controlling film Eq. (11) [5].

$$\frac{1}{U_0 \cdot A_0} = \frac{1}{h_s \cdot A_s} + \frac{R_s}{A_s} + \frac{\ln(D_0/D_i)}{2\pi \cdot k_w \cdot L} + \frac{R_t}{A_t} + \frac{1}{h_t \cdot A_t} \quad (11)$$

2.1. Hydraulic design

In this section is presented equations for the pressure drop for the shell side and tubes side, Eq. (12) showed the pressure drop for the shell side [6].

$$\Delta P_s = [(N_b - 1) \Delta P_{b,id} \cdot \zeta_B + N_b \cdot \Delta P_{b,id}] \zeta_L + 2 \cdot \Delta P_{b,id} \left(1 + \frac{N_{r,cw}}{N_{r,cc}} \right) \zeta_B \cdot \zeta_S \quad (12)$$

In the above equation is taken into account the pressure drop in the crossflow sections, in the windows of the baffles. This equation is affected by a correction coefficient group.

- ζ_L : Correction factor for the tubes-to-baffle and baffle-to-shell leakage (A and E) streams. Usually vary from 0.4 to 0.5, although lower values are possible with small baffle spacing.
- ζ_B : Correction factor for bypass flow (C and F) streams, depending of type construction and number of sealing strips, variation range is from 0.5 to 0.8.
- ζ_S : Correction factor for inlet and outlet sections, having unequal baffle spacing from that of the central section. This varies from 0.5 to 2.

The pressure drop for tubes side is estimated for Eq. (13) presented in [7].

$$\Delta P_t = \frac{f_t \cdot L \cdot G_t^2 \cdot N_p}{2\rho_t \cdot \phi_t} + \frac{4G_t^2 \cdot N_p}{2\rho_t} \quad (13)$$

In Eq. (11) the first term corresponds to the pressure drop caused by fluid friction inside the tubes and the second term takes into account the change in direction of fluid (U-Tubes), not taken into account the losses in the inlet and outlet nozzles.

The Bell-Delaware design methodology is widely used for estimated heat transfer and pressured drop for the shell side [8-14].

3. Optimization design of shell and tubes exchanger

To optimize the previously proposed design is implemented an elitist genetic algorithm NSGA-II in Octave. Minimizing the number of entransy dissipation and total cost, subject to the following set of constraints.

- Length of the tubes in the range 1.4 to 1.6 m.
- Cutting percent deflectors 15-35.
- Outside tubes diameter in the range 0.0125 to 0.0508 m.
- Fraction of the spacing of the baffles and the shell inside diameter of 0.2 to 1.
- Number of tubes in the range 150 to 230.
- Pressure drop in the shell side that less 30 kPa.
- Pressure drop in the tubes side that less 1.5 kPa.
- The fuel outlet temperature in the range of 118°C to 134°C.

This set of constraints respond to geometric constraints on where the equipment is installed, tubes standard [15], operating conditions and common practices in the design of heat transfer equipment. A major constraint is the viscosity of the fuel outlet which should be in the range of 12 to 18 cSt, this corresponds to a temperature range of 134 to 118°C.

3.1. Objective functions

Traditionally the optimization of thermal systems is supported by exergy principles described in [16-17], these authors define the principle of minimum energy dissipation and minimum entropy generation [18]. Based in those principle, for a thermal system in steady state the entropy generation should be minimum. According to [12], the above definition is not in correspondence with the optimum heat exchanger. Bejan [19-21] has studied the exergy loss for the heat transfer of a fluid across a finite temperature difference in a conduct with friction, defining the entropy generation number. The analysis applying the result of the mentioned study in a counter flow heat exchanger showed that entropy generation number approaches to zero in two limits: when the effectiveness approaches unity $\varepsilon \rightarrow 1$ or the number of transfer units approaching to infinity $NTU \rightarrow \infty$, which represents the ideal limit of zero driving temperature difference, and when effectiveness approaches zero $\varepsilon \rightarrow 0$ or number transfer unit approaches to zero $NTU \rightarrow 0$, which represent heat transfer surface approaching to zero. As shown in Figure 3 the number of generation of entropy has a symmetrical behaviour, where not always the minimum entropy generation number corresponds to a maximum effectiveness. Bejan called this phenomenon the paradox of entropy generation. For this problem, the entropy generation number is not an appropriate criterion for optimizing the design of heat exchangers. About the year 2000, in analogy to the electrical conduction, a new principle called “Entransy” arises [22], this property is the ability of the material to transfer heat. In this paper the first objective function is entransy dissipation number, for heat exchanges in single phase the equations are presented in [23]. In the case study presented a phase change of the fluid occur. And single phase equations are not applicable.

Taking from [23] the equation for the cold fluid of single phase and developing the equation for hot fluid with phase change, the equations for entransy balance of the heat exchanger can be defined according to Eq. (14).

$$\int_{T_{c,i}}^{T_{c,o}} \dot{m}_c C_{p,c} T_c dT_c = - \int_{h_i}^{h_o} \dot{m}_h T_h dh + \dot{G}_{diss\Delta T} \quad (14)$$

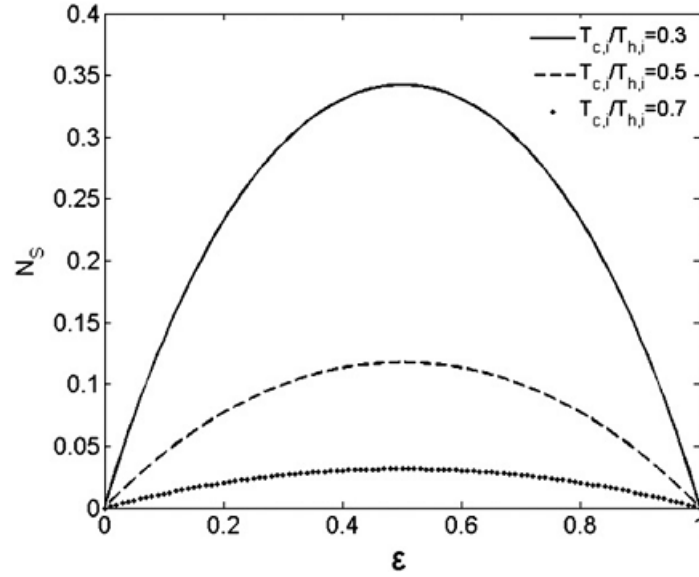


Fig. 3. Relationship between N_s vs. ε for a counterflow heat exchanger.

Integrating from inlet to outlet the above equation and grouping both members is obtained the entransy dissipation for heat transfer Eq. (15).

$$\dot{G}_{diss\Delta T} = \dot{m}_h T_h (h_i - h_o) + \frac{1}{2} \dot{m}_c C_{p,c} (T_{c,i}^2 - T_{c,o}^2) \quad (15)$$

The entransy dissipation for the cold fluid of single phase and entransy dissipation for the hot fluid with phase change, corresponding to the irreversibility introduced by fluid friction in the process of heat transfer is quantified by Eq. (16).

$$\dot{G}_{diss\Delta P} = \dot{m}_c \frac{\Delta P_s (T_{c,o} - T_{c,i})}{\rho_s \ln\left(\frac{T_{c,o}}{T_{c,i}}\right)} - \dot{m}_h p_s \bar{v} \ln\left(\frac{P_o}{P_i}\right) \quad (16)$$

Finally is obtained, the dimensionless dissipation entransy number for heat transfer and friction flow according to Eq. (17), Eq. (18) and the total entransy dissipation number Eq. (19).

$$G^*_{diss\Delta T} = \frac{\dot{G}_{diss\Delta T}}{\dot{q}(T_{h,i} - T_{c,i})} \quad (17)$$

$$G^*_{diss\Delta P} = \frac{\dot{G}_{diss\Delta P}}{\dot{q}(T_{h,i} - T_{c,i})} \quad (18)$$

$$G^*_{dissTotal} = G^*_{diss\Delta T} + G^*_{diss\Delta P} \quad (19)$$

In the Eq. (17) and Eq. (18) the term $\dot{q}(T_{h,i} - T_{c,i})$ is the maximum entransy dissipation.

The second objective function is the total cost Eq. (20), according to [24] this estimates the cost of initial investment Eq. (21) and operating cost Eq. (22).

$$TC = PC \frac{i(1+i)^n}{(1+i)^n - 1} + OC \quad (20)$$

$$PC = 3,28 \cdot 10^4 \left(\frac{A_s}{80}\right)^{0,68} \delta_M \delta_P \delta_T \quad (21)$$

$$OC = \frac{(E_s + E_t)_{op} \cdot ec}{1000} \quad (22)$$

The corrections factors for Eq. (19) are showed in table 1 and electricity price (ec) assumed is 0.15(USD/kW · h).

Table 1. The capital cost factors.

Material of construction	Correction factor δ_M
CS shell and tubes	1
CS shell, aluminium tubes	1.3
CS shell, monel tubes	2.1
CS shell, SS tubes	1.7
SS shell and tubes	2.9
Design pressure (Pa)	Correction factor δ_p
1000	2
10 000	1.3
50 000-700 000	1
5 000 000	1.5
10 000 000	1.9
Design temperature (°C)	Correction factor δ_T
0-100	1
300	1.6
500	2.1

4. Results and discussions

Applying the principles of entransy dissipation and the empirical equations presented above for total cost estimation an elitist genetic algorithm NSGA-II was implemented. Pareto front shown in figure 4 is obtained. For this case, in advantage over single-objective optimization, the multi-objective optimization displays a set of solutions, bean the Pareto front a versatile tool for this applications, although in some cases this is a problem because of necessary decisions making process to select the best solution for the design.

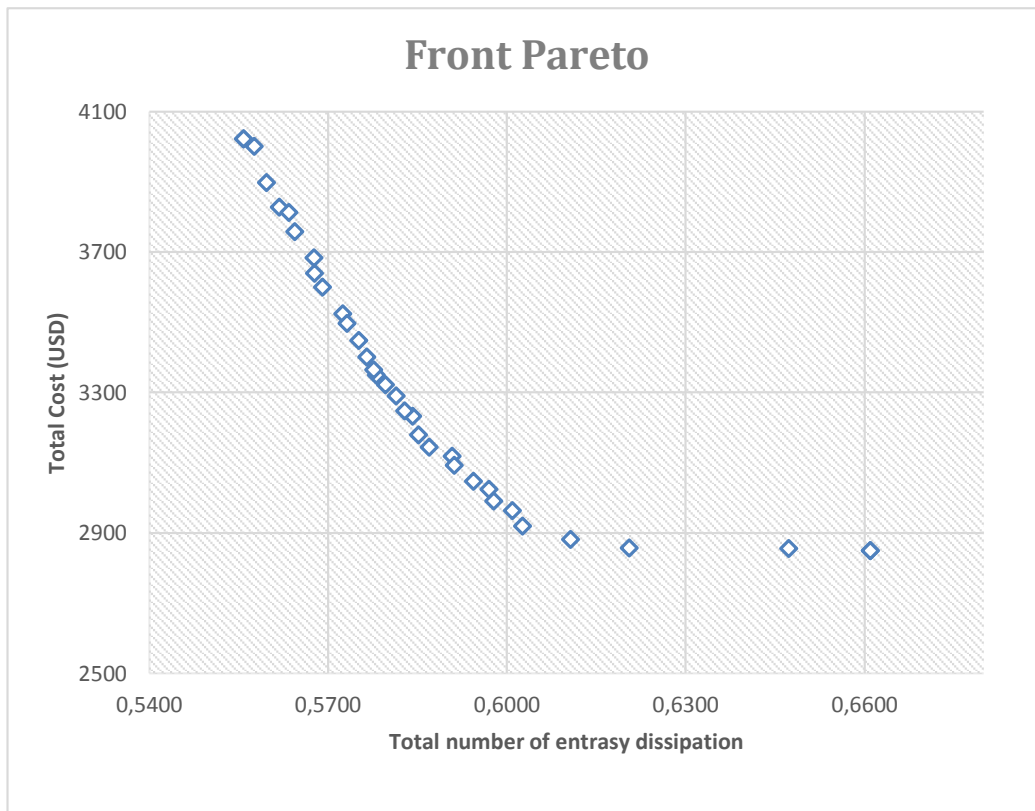


Fig. 4. Pareto front for the optimization.

According to the Pareto front obtained, the total number of entransy dissipation decrease as costs increase. This occur because the NTU depends largely on the overall coefficient of heat transfer and the heat transfer surface, and also due to the effectiveness depends on the number of units transferred. High effectiveness corresponds to an area of large heat transfer or high pressure drop which would make the cost increases.

In order to make the best selection is recommended the following criteria, select the equipment with the highest heat transfer rate at the minimum cost. For this case is used the graph shown in Figure 5, where it can be seen that the best solutions are those where the fuel outlet temperature is about 125°C. These heat exchangers are those with a high rate of heat transfer at minimal cost. In Table 2 is showed the decisions vector for the best solutions according to figure 5, in Table 3 a set of parameters of interest of the thermal and hydraulic performance are given.

Table 2. Vector decisions for the best solutions.

D_0, m	L, m	$L_c, \%$	B_s	N_T
0.01588	1.601	19.34	0.34	150
0.01588	1.620	17.99	0.27	151
0.01588	1.646	18.84	0.21	151
0.01588	1.632	17.96	0.21	156

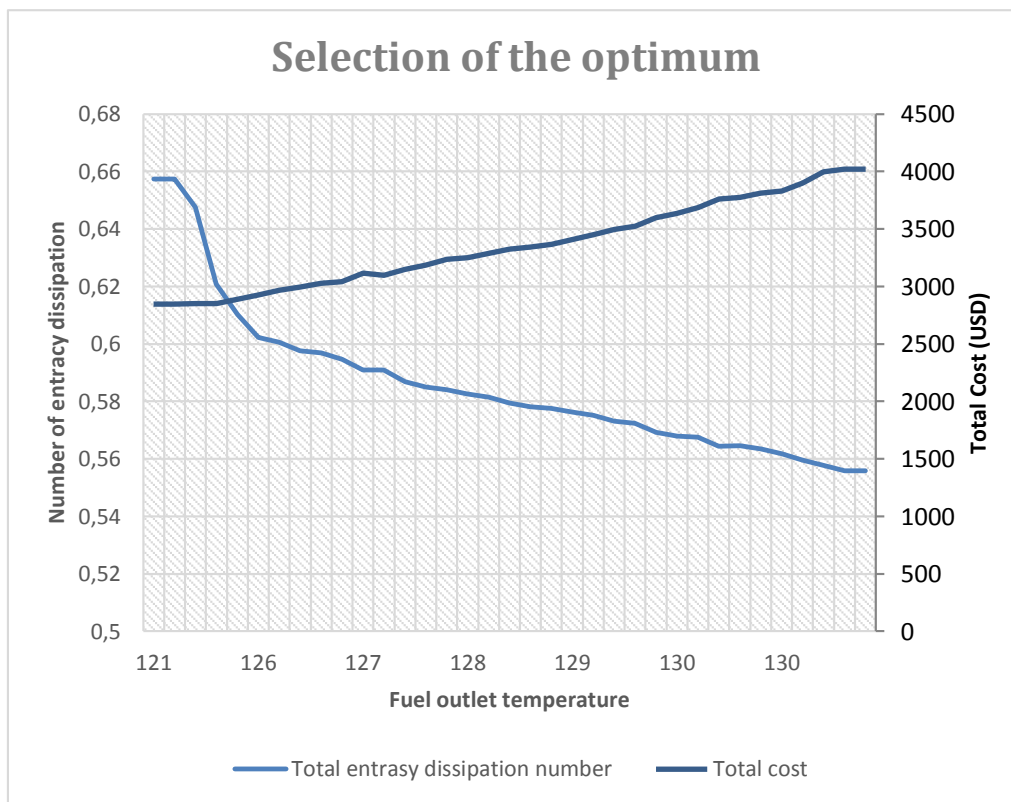


Fig. 5. Selection of the optimum design.

According to the previously arguments the best effectiveness of the heat exchangers is synonymous of a less dissipation of entransy and low number of entransy dissipation. The ideal selection for this operating conditions correspond to a heat exchanger with the maximum effectiveness, but it was selected a design with an effectiveness equal to 0.76. This selection was made taking in to account not only operating conditions, but also maximum effectiveness involving the minimal cost was considered. In figure 6 is showed the dependence of the entransy number dissipation and efficiency

for all solutions offered by Pareto front. Analysing figure 6 it can be seen, that more effectiveness correspond to lower number of entransy dissipation. The main geometrical parameters for the selected design are shown in Table 4.

Table 3. Principal performance thermal-hydraulic parameter.

G_{total}^*	TC, USD	$T_{c,o}, ^\circ C$	ε	NTU	$U_c, \frac{W}{(m^2 \cdot ^\circ C)}$	$\Delta P_s, kPa$	$\Delta P_s, kPa$
0,6208	2851	125	0,76	1,42	360	8,53	0,18
0,6103	2887	126	0,78	1,52	377	9,60	0,18
0,6023	2926	126	0,80	1,60	390	23,00	0,18
0,6005	2969	127	0,80	1,61	384	13,68	0,17

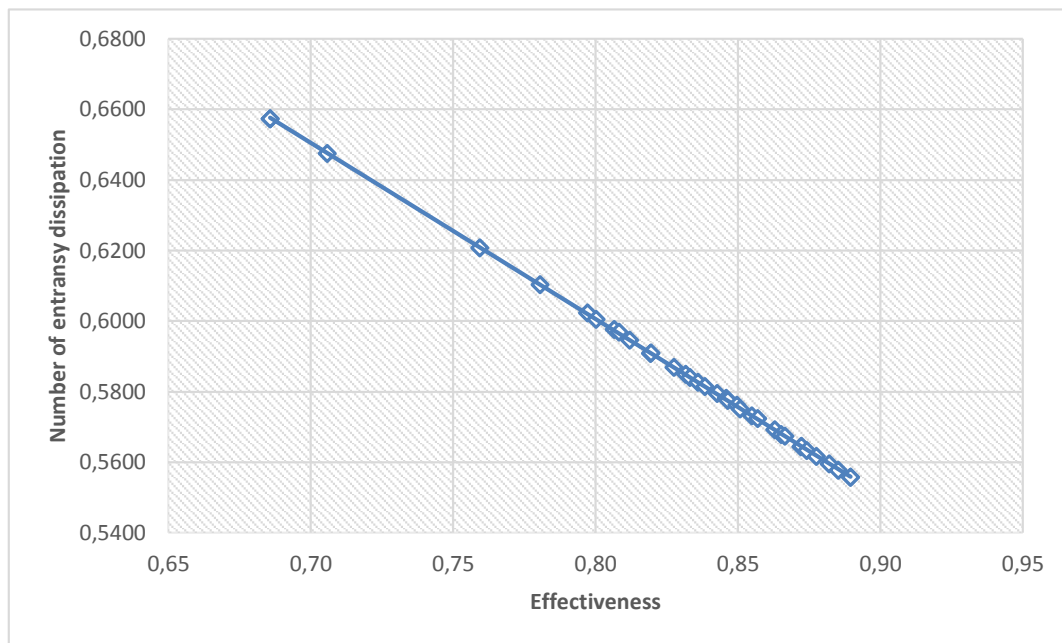


Fig. 6. Dependence number entransy dissipation and effectiveness.

Table 4. The main geometrical parameter.

D_0, m	L, m	$L_c, \%$	N_T	L_{bc}, m	D_S, m	N_B	N_P	P_t, m
0.01588	1.601	19.34	150	0.101	0.2996	15	2	0.01985

5. Conclusions

In this paper, the entransy dissipation theory is used for a multi-objective optimization, instead of the principle of minimum entropy generation. A set of solutions was obtained, the solutions found matches with the design principles found in the consulted literature, in all cases increasing effectiveness decreases the number of entransy dissipation. Finally, for the designs obtained is selected the equipment with maximum heat transfer speed and minimum cost, this equipment ensures a fuel outlet temperature in the range of operating conditions.

Nomenclature

A heat transfer surface, m^2

C thermal capacitance, $W/^\circ C$

c_p specific heat, $W/(kg \cdot ^\circ C)$

CS carbon steel
 D_s shell inside diameter, m
 E pumping power, kW
 E_c electric cost, USD/kW · h
 f friction factor
 G fluid mass velocity, kg/(m² · s)
 $\dot{G}_{diss\Delta T}$ entransy dissipation for heat conduction, W · °C
 $\dot{G}_{diss\Delta P}$ entransy dissipation for pressure drop, W · °C
 G^* entransy dissipation number
 h specific enthalpy, W/kg
 HFO Heavy Fuel Oil
 h_{ideal} ideal heat transfer coefficient, W/(m² · °C)
 k thermal conductivity, W/(m · °C)
 \dot{m} mass flow, kg/s
 N_b number of baffle
 NTU number transfer units
 N_p number of passes
 N_r Number of effective tubes rows
 L Longitude, m
 OC operation cost, USD
 op operate period, year
 PC capital cost, USD
 P_t tube pitch, m
 P_r Prandalt number
 \dot{q} heat flow, W
 T temperature, °C
 R Fouling factor, m² · °C/W
 U_0 Overall heat transfer coefficient, W/m²
 ΔP pressure drop, Pa
 $\Delta P_{b,id}$ ideal pressure drop for tube bank, Pa

Greek symbols

ε effectiveness
 ϕ viscous correction coefficient
 ρ density, kg/m³

Subscripts and superscripts

c,o cold outlet
 c,i cold inlet
 cc crossed during flow through one crossflow section
 cw during flow through one window zone in a segmental baffled shell-and-tube heat exchanger
 fg phase change
 h hot side
 min minimum

max maximum
l liquid
t tubes side
sat saturation
v steam
w wall

References

1. De Cuba, A.E., *Oficina Nacional de Estadísticas*. Various years. Havana, 2013.
2. Zhang, J.-F., Y.-L. He, and W.-Q. Tao, *3D numerical simulation on shell-and-tube heat exchangers with middle-overlapped helical baffles and continuous baffles—Part I: Numerical model and results of whole heat exchanger with middle-overlapped helical baffles*. *International Journal of Heat and Mass Transfer*, 2009. **52**(23): p. 5371-5380.
3. Master, B.I., K.S. Chunangad, and V. Pushpanathan, *Fouling mitigation using helixchanger heat exchangers*. 2003.
4. Incropera, F.P., *Introduction to heat transfer*. 2011: John Wiley & Sons.
5. Cengel, Y.A., S. Klein, and W. Beckman, *Heat transfer: a practical approach*. 1998.
6. Shah, R.K. and D.P. Sekulic, *Fundamentals of heat exchanger design*. 2003: John Wiley & Sons.
7. Kuppan, T., *Heat exchanger design handbook, 2000*, Marcel Dekker, Inc.
8. Fesanghary, M., E. Damangir, and I. Soleimani, *Design optimization of shell and tube heat exchangers using global sensitivity analysis and harmony search algorithm*. *Applied Thermal Engineering*, 2009. **29**(5): p. 1026-1031.
9. Guo, J. and M. Xu, *The application of entransy dissipation theory in optimization design of heat exchanger*. *Applied Thermal Engineering*, 2012. **36**: p. 227-235.
10. Guo, J., M. Xu, and L. Cheng, *The application of field synergy number in shell-and-tube heat exchanger optimization design*. *Applied Energy*, 2009. **86**: p. 2079-2087.
11. Leoug, K., K. Toh, and Y. Leong, *Shell and tube heat exchanger design software for educational applications*. *International Journal of Engineering Education*, 1998. **14**(3): p. 217-224.
12. Qian, X. and Z. Li, *Analysis of entransy dissipation in heat exchangers*. *International Journal of Thermal Sciences*, 2011. **50**(4): p. 608-614.
13. Sanaye, S. and H. Hajabdollahi, *Multi-objective optimization of shell and tube heat exchangers*. *Applied Thermal Engineering*, 2010. **30**(14): p. 1937-1945.
14. Wildi - Tremblay, P. and L. Gosselin, *Minimizing shell - and - tube heat exchanger cost with genetic algorithms and considering maintenance*. *International journal of energy research*, 2007. **31**(9): p. 867-885.
15. Association, T.E.M., *Standards of Tubular Exchanger Manufacturers Association*. 1959: TEMA.
16. Machlup, S. and L. Onsager, *Fluctuations and irreversible process. II. Systems with kinetic energy*. *Physical Review*, 1953. **91**(6): p. 1512.
17. Onsager, L., *Reciprocal relations in irreversible processes. II*. *Physical Review*, 1931. **38**(12): p. 2265.
18. Prigogine, I., *Introduction to Thermodynamics of Irreversible Processes (3rd edn.) Interscience*. New York, 1967: p. 23-25.
19. Bejan, A., *The concept of irreversibility in heat exchanger design: counterflow heat exchangers for gas-to-gas applications*. *Journal of heat transfer*, 1977. **99**(3): p. 374-380.
20. Bejan, A., *General criterion for rating heat-exchanger performance*. *International Journal of Heat and Mass Transfer*, 1978. **21**(5): p. 655-658.
21. Bejan, A., *Second-law analysis in heat transfer and thermal design*. *Adv. Heat Transfer*;(United States), 1982. **15**.

22. Guo, Z.-Y., H.-Y. Zhu, and X.-G. Liang, *Entransy—a physical quantity describing heat transfer ability*. International Journal of Heat and Mass Transfer, 2007. **50**(13): p. 2545-2556.
23. Xu, M., *The thermodynamic basis of entransy and entransy dissipation*. Energy, 2011. **36**(7): p. 4272-4277.
24. Allen, B. and L. Gosselin, *Optimal geometry and flow arrangement for minimizing the cost of shell - and - tube condensers*. International Journal of Energy Research, 2008. **32**(10): p. 958-969.